Coupled Simulations of RF Effects on Tearing Modes

S.E. Kruger[1], T.G. Jenkins[1], E.D. Held[2], J.J. Ramos[3], J. King[1], D.D. Schnack[4] and R.W. Harvey[5]

[1]Tech-X Corporation, Boulder, CO 80303 USA
[2]Utah State University, Logan, Utah USA
[3]Massachusetts Institute of Technology, Cambridge, MA USA
[4]University of Wisconsin-Madison, Madison, WI USA
[5]CompX Corporation, Del Mar, CA USA

Corresponding Author: kruger@txcorp.com

Abstract:

We present integrated feedback simulations of neoclassical tearing modes in tokamak plasmas. The implementation relies on the NIMROD and GENRAY codes, along with new codes for calculating a local quasilinear operator, and for performing the code coupling. The mathematical formulation relies on the formulation of a third-order electron drift-kinetic equation that captures the bootstrap current effects and is consistent with ECRF-driven kinetic distortion effects such as the Fisch-Boozer and Ohkawa current drives. Numerically solving the drift-kinetic equation relies on a new high-order continuum discretization scheme suitable for solving the equation in the presence of a macroscopic three-dimensional magnetic field. Implementing these new kinetic closures implicitly, along with the drift-kinetic terms, provides many numerical challenges and requires careful verification.

1 Introduction

Electron cyclotron current drive (ECRF) has successfully been used to stabilize tearing modes in multiple experiments. Such experiments may either rely on sophisticated active feedback control to locate and drive time-modulated current in island O-points of the rotating plasma, or use continuously driven current to stabilize the mode. Using these approaches, considerable efforts have been made to determine an optimal strategy for the mitigation and control of magnetic islands in ITER [1]. Theoretical calculations using ECRF-induced modifications to the Rutherford equation show that if the driven current is perfectly localized at the O-point of the island, then less than one percent of the plasma current is needed for stabilization [2]. Computational modeling can offer detailed exploration of feedback control schemes in a way that is not possible with experimental devices. Because the O-point and frequency of the island are known, it is possible to implement a "perfect" control system that minimizes the power needed for

the ECRF sources while accounting for the slow evolution of the plasma equilibrium on transport timescales. This is important because the movement of the rational surfaces in response to ECRF sources explains [3] previously calculated stability results [4]. Using synthetic diagnostics, experimentally relevant feedback systems can be implemented, and by comparing the experimental feedback system with the "perfect" system, approaches for optimizing RF feedback systems can be investigated.

2 Mathematical formulation

To perform these investigations, a mathematical and computational formalism is needed. Unlike previous models [5] which used a quasi-analytic model for the incorporation of ECRF sources, a newer, more formal approach [6,7,8] is used here. Like all plasma fluid theories, the approach takes moments of the kinetic distribution function [9], but leverages the significant work in improving the accuracy of fluid theories for the nearly collisionless regimes in modern tokamaks that has occurred over the past decade.

Closed systems of fluid equations are typically derived by first taking velocity moments of the full kinetic equation, followed by an ordering of terms in the resultant moment equations [10]. To use a kinetic equation to close the system, one may then use a kinetic equation whose terms are ordered in a manner consistent with the ordered fluid theories. However, previous approaches have demonstrated inconsistency in that moments of the ordered-kinetic equation did not agree with the ordered moments of the full kinetic equation. In Ref. [10], a drift-kinetic equation is developed to eliminate this inconsistency. The drift-kinetic equation is derived in a moving reference frame and is accurate to first order in the FLR expansion. It is valid for fully electromagnetic nonlinear dynamics, sonic macroscopic flows, and far-from-Maxwellian distribution functions. Its consistency therefore provides a sound basis for deriving closures for the parallel heat flux and stress tensors, as well as for the inclusion of terms which arise from ECRF effects.

Development of fluid equations in the presence of ECRF relies on the observation [7] that ECRF only slightly modifies the distribution function; thus, the induced distortion of the distribution function away from the zeroth-order Maxwellian is on the same order as the distortions required to close the fluid moment equations. One may then use a Chapman-Enskog-like approach ([12,6-8]), to derive an equation for the kinetic distortion away from a *dynamic* Maxwellian:

$$f_e(v'_\parallel, v'_\perp, \chi, \mathbf{x}, t) \;=\; \bar{f}_e(v'_\parallel, v'_\perp, \mathbf{x}, t) \;+\; \tilde{f}_{NMe}(v'_\parallel, v'_\perp, \chi, \mathbf{x}, t)\;, \tag{1}$$

Unlike the delta-f method used in gyrokinetics, the use of a dynamic Maxwellian enables the evolution of the Maxwellian over long time scales to be described by moment equations. Using this approach and a realistic low-collisionality ordering scheme, a third-order electron drift-kinetic equation was derived [6], together with a similar equation for ion

closures as well [11]. The form is given by:

$$\frac{\partial \bar{f}_{NMe}}{\partial t} + \cos\chi \left(v' \mathbf{b} \cdot \frac{\partial \bar{f}_{NMe}}{\partial \mathbf{x}} + v_{the}^2 \mathbf{b} \cdot \nabla \ln n \, \frac{\partial \bar{f}_{NMe}}{\partial v'} \right) \quad (2)$$

$$- \frac{\sin\chi}{v'} \left(v_{the}^2 \mathbf{b} \cdot \nabla \ln n - \frac{v'^2}{2} \mathbf{b} \cdot \nabla \ln B \right) \frac{\partial \bar{f}_{NMe}}{\partial \chi} = \Bigg\{ \cos\chi \, \frac{v'}{2T_e} \left(5 - \frac{v'^2}{v_{the}^2} \right) \mathbf{b} \cdot \nabla T_e$$

$$+ \cos\chi \, \frac{v'}{nT_e} \, \mathbf{b} \cdot \left[\frac{2}{3} \nabla (p_{e\parallel} - p_{e\perp}) - \left(p_{e\parallel} - p_{e\perp} \right) \nabla \ln B - \mathbf{F}_e^{coll} \right]$$

$$+ P_2(\cos\chi) \, \frac{v'^2}{3v_{the}^2} \Big(\nabla \cdot \mathbf{u}_e - 3\mathbf{b} \cdot [(\mathbf{b} \cdot \nabla)\mathbf{u}_e] \Big) \, \frac{1}{3nT_e} \left(\frac{v'^2}{v_{the}^2} - 3 \right) \left[\nabla \cdot (q_{e\parallel} \mathbf{b}) - G_e^{coll} \right]$$

$$+ \frac{1}{6eB} \left[2P_2(\cos\chi) \frac{v'^2}{v_{the}^2} \left(\frac{v'^2}{v_{the}^2} - 5 \right) + \frac{v'^4}{v_{the}^4} - 10 \frac{v'^2}{v_{the}^2} + 15 \right] (\mathbf{b} \times \boldsymbol{\kappa}) \cdot \nabla T_e$$

$$+ \frac{1}{6eB} \left[-P_2(\cos\chi) \frac{v'^2}{v_{the}^2} \left(\frac{v'^2}{v_{the}^2} - 5 \right) + \frac{v'^4}{v_{the}^4} - 10 \frac{v'^2}{v_{the}^2} + 15 \right] (\mathbf{b} \times \nabla \ln B) \cdot \nabla T_e$$

$$+ P_2(\cos\chi) \, \frac{v'^2}{3eBv_{the}^2} (\mathbf{b} \times \nabla \ln n) \cdot \nabla T_e \Bigg\} f_{Me} + \langle C_{ee}[f_e, f_e] + C_{e\iota}[f_e, f_\iota] \rangle_\alpha \quad (3)$$

where P_l denote the Legendre polynomials, i.e. $P_2(z) = 3z^2/2 - 1/2$. A similar equation for ions can be found in Ref. [8]. This novel form features rigorous Fokker-Planck collision operators and can recover the neoclassical results of the electron banana regime. It also has the property of automatically guaranteeing that the distribution function perturbation never contributes to the density, flow velocity or temperature fluid moments, thus facilitating the compatibility of the closure with the fluid equations. This new formalism provides the physics of the bootstrap current and Landau damping in arbitrary geometry, as required for tearing mode evolution.

The inclusion of ECRF terms requires the addition of two additional terms to the fluid equations, namely, sources for the induced electron momentum and heat. These terms may be written respectively as ([13]):

$$\mathbf{F}_\alpha^{RF} = \mathbf{k}_{rs} H_\alpha; \qquad S_\alpha^{RF} = \omega H_\alpha \quad (4)$$

where the quantity H_α is defined as

$$H_\alpha \equiv \frac{\epsilon_0}{2} \mathbf{E}_s^* \cdot \chi_\alpha^a(\mathbf{k}, \omega) \cdot \mathbf{E}_s \langle e^{i(\psi - \psi^*)} \rangle \, . \quad (5)$$

and contains the physics responsible for the transfer of RF power to the MHD plasma. Here $\mathbf{k}_{rs}$ is the real part of the wave vector of the ECRF and ω is its frequency; both

quantities can be derived by taking spatial and temporal gradients of the RF phase function $\psi(\mathbf{x}, t)$. The spatiotemporal variation of H_α on the MHD scale is determined by the background density, temperature, velocity, and magnetic field profiles. In the vicinity of the resonance (the only region where its effects are manifest in the extended MHD dynamics), it can be expressed as

$$H_\alpha = \frac{\epsilon_0}{4} \sum_{n=-\infty}^{\infty} \frac{\omega_{p\alpha s}^2}{\omega^2} e^{-\lambda_{\alpha s}} \xi_{0s} \sqrt{\pi} e^{-\xi_{nrs}^2} \times$$

$$\left[[I_n(\lambda_{\alpha s}) - I_{n+1}(\lambda_{\alpha s})] \left(2\lambda_{\alpha s} |E_{ys}|^2 + n \left| E_{xs} - iE_{ys} + \frac{\sqrt{\lambda_{\alpha s}}(\omega - n\Omega_{\alpha s}) E_{zs}}{n k_{\parallel s} v_{t\alpha s}} \right|^2 \right) \right.$$

$$\left. + [I_n(\lambda_{\alpha s}) - I_{n-1}(\lambda_{\alpha s})] \left(2\lambda_{\alpha s} |E_{ys}|^2 - n \left| E_{xs} + iE_{ys} + \frac{\sqrt{\lambda_{\alpha s}}(\omega - n\Omega_{\alpha s}) E_{zs}}{n k_{\parallel s} v_{t\alpha s}} \right|^2 \right) \right] . \quad (6)$$

Here, ξ_{nrs} is the real part of the conventional argument of the plasma dispersion function, I_n is the modified Bessel function, and the Stix coordinates [14] are used for the components of wave fields. This equation expresses the ECRF source terms in a form amenable to numerical implementation. The ECRF deposition also alters the kinetic distortion and thus the closure calculation; hence, Eq. 3 requires additional terms to capture these effects. These additional terms may be found in Refs. [6,7].

3 Numerical Implementation: Beyond MHD

To numerically implement this closure, a new continuum discretization scheme for the distribution function has been developed. Unlike previously developed kinetic discretization schemes for neoclassical and turbulence codes, this scheme was developed accounting for the unique issues of distortions in the presence of a tearing mode. The scheme is developed by changing the velocity variables of Eq. 1 to speed and pitch angle. The speed variable contains no derivatives and is thus amenable to a simple, parallelizable collocation scheme. To represent the pitch angle, high-order finite elements are used. The use of high-order finite elements gives the advantage of polynomial convergence similar to that used in polynomial expansions while allowing packing near sharp features (such as those caused by electron-ion collisions). As shown in Figure 1, this scheme is successfully able to calculate the bootstrap current when compared to the NEO code [14], which is only axisymmetric and per flux surface. For the comparison the Hazeltine form of the drift kinetic equation [15] was used to minimize the differences with NEO. Unlike NEO, which was written assuming an axisymmetric Grad-Shafranov equilibrium and thus can calculate solutions on a single flux surface, this calculation was done over the entire NIMROD grid using NIMROD fields.

The closures must be integrated in time along with the temporal discretization schemes that are also important when solving the full set of fluid equations, including the drift ordered terms [10]. For example, a well known result from drift-reduced MHD is that

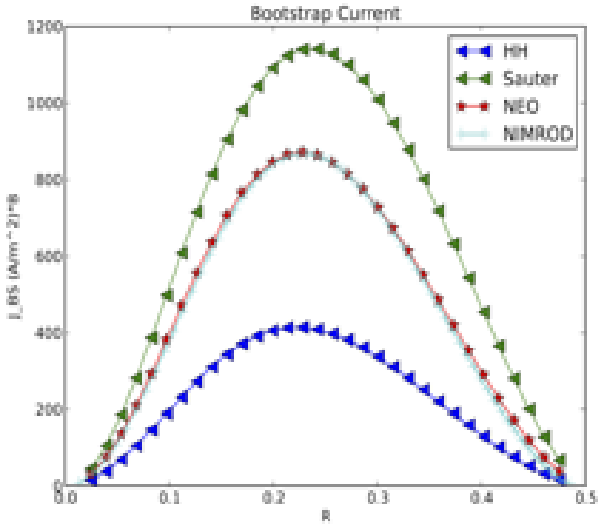

FIG. 1: A comparison of NIMROD's calculation of the bootstrap current with the NEO code [14] shows excellent agreement, and better than the large aspect-ratio analytic formulas.

the diamagnetic drift has a stabilizing influence on tearing modes [16]. Our unreduced extended-MHD computations with the NIMROD code include these diamagnetic effects [17]; however, the decrease in the growth rate from NIMROD large-guide-field slab computations is significantly less than the expected analytical result as seen in Figure 2. New analytics, following work of Refs. [18] which explored the regime where diffusion of the parallel magnetic field is important, have been developed to explore this experimentally-relevant regime. Computational diagnostics are used to examine terms in the flux evolution equation believed to be important and agree with the analytic theory explaining the the discrepancy between extended MHD and drift-reduced MHD.

4 Numerical Implementation: Coupled Simulations

To incorporate the RF sources accurately, the GENRAY code is used to model RF propagation and power deposition. As the NIMROD code advances, its axisymmetric fields are provided to GENRAY, which is running concurrently on a separate group of processors. GENRAY then provides the local, eikonal electric fields along the rays. A new code creates a three-dimensional grid of hexagonal prisms around the ray points in order to integrate the fields and construct the quasilinear operator; knowledge of the volume associated with each ray point is necessary to transform the GENRAY data (discrete solutions along individual ray trajectories) into NIMROD's continuous fluid representation. By taking moments of the quasilinear operator, the fluid moments and information needed for the closure calculations can be obtained on the three-dimensional grid. Because the quasilinear operator is calculated locally and is not toroidally or bounce-averaged, significantly

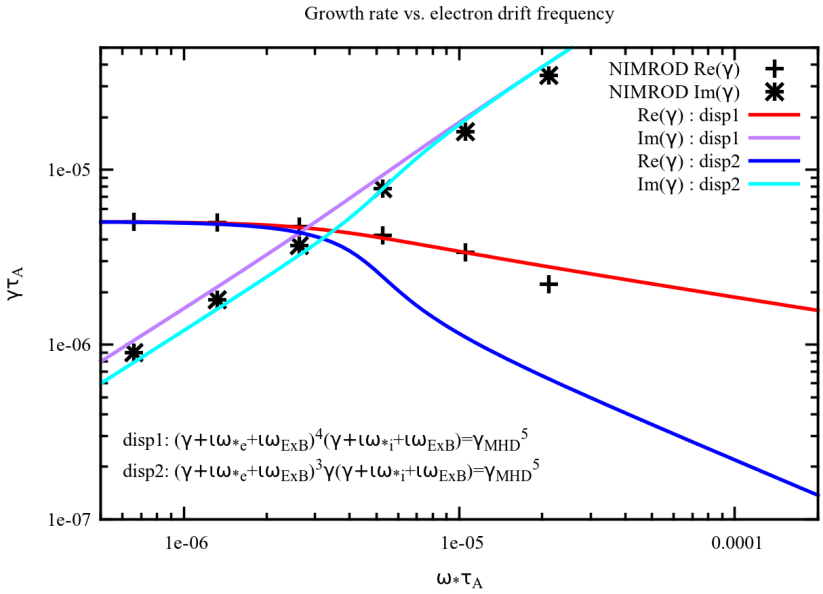

FIG. 2: Growth rate and real frequency given by NIMROD does not agree with the typical dispersion relation for drift-tearing modes.

more rays than typical transport simulations employ are required to ensure convergence of the RF sources.

In tandem with the concurrently running fluid and RF codes, we have developed a synthetic plasma control system and are tuning this system to optimize the physics of RF/MHD interaction. The control system monitors NIMROD's synthetic Mirnov coil diagnostic, enabling the detection and identification of tearing modes as they develop. Threshold values for the diagnostic output are set to determine when the mode is large enough that RF should be employed (in our case, by communicating its presence to NIMROD) or small enough that it can be discontinued; the position of the RF beam relative to the island O-point can also be adjusted through adjustments to the steering angle (corresponding to mirror adjustment in actual experiments).

An example simulation (Figure 3) shows that when the island size exceeds a threshold set by the synthetic control system, the RF is injected and the island size starts to decrease. In this case, the mode does not stabilize before the RF is turned off. For this simulation, a "perfect" feedback scheme was implemented by using a fieldline integration code to determine the O-point location of the rotating island.

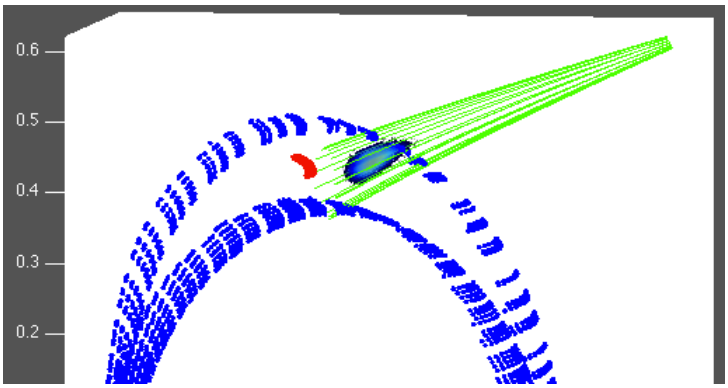

FIG. 3: Modeling the deposition of ECRF into the plasma using NIMROD and GENRAY requires the transfer of discrete ray tracing solutions (along individual trajectories) to the continuous representation of the NIMROD grid.

5 Summary

The results of this paper demonstrate the evolution of the extended MHD efforts toward more complex 5-dimensional continuum, drift-kinetic codes with the ability to capture kinetic dynamics on long time scales. Unlike other continuum drift-kinetic codes such as NEO, we include three-dimensional effects for arbitrary magnetic fields (including stochastic magnetic fields). Unlike the gyrokinetic codes, we include the full linearized force operator which is needed to obtain accurate stability thresholds for long-wavelength instabilities. The mathematical and numerical framework has also allowed the development of a first-principles integration with ECRF ray-tracing codes. Achieving first-principles solutions for long-wavelength instabilities over long time scales and in nearly collisionless plasmas has presented many analytic and numerical challenges. As demonstrated in this paper, the significant progress over the past five years has developed tools of unprecedented accuracy and power for modeling tokamak discharges.

References

[1] R. LaHaye, R. Prater, R.J. Buttery, et al., Nuclear Fusion **46**, 451 (2006).

[2] C.C. Hegna and J.D. Callen, Phys. Plasmas **4**, 2940 (1997).

[3] T.G. Jenkins, S.E. Kruger, C.C. Hegna, et al., Phys. Plasmas **17** (2010).

[4] A. Pletzer and F.W. Perkins, Phys. Plasmas **6**, 1589 (1999).

[5] Q. Yu, S. Günter, G. Giruzzi, et al., Phys. Plasmas **7**, 312 (2000).

[6] J. J. Ramos, Phys. Plasmas **17**, 082502 (2010);

[7] C. C. Hegna and J. D. Callen, Phys. Plasmas **16**, 112501 (2009).

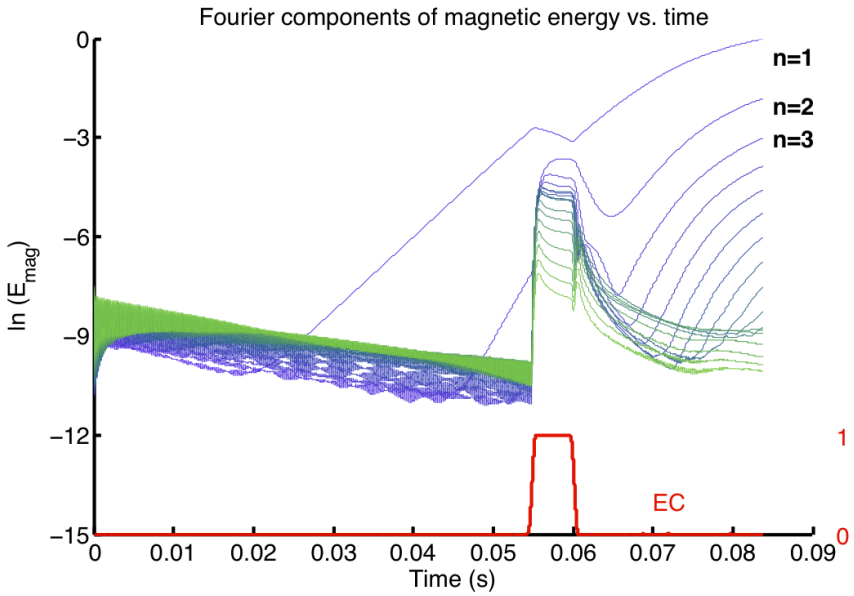

FIG. 4: Suppression of a tearing mode in response to injected ECRF; energy in the individual Fourier components corresponds roughly to mode energy. In this case, the RF is perfectly aligned with the O-point and suppression occurs rapidly; mode growth resumes when the ECRF is shut off.

[8] J.J. Ramos, Phys. Plasmas **18**, 102506 (2011) .

[9] S. I. Braginskii, Transport Processes in a Plasma, edited by M. A. Leontovich Consultants Bureau, New York, 1965, Vol. 1.

[10] D.D. Schnack, D.C. Barnes, D.P. Brennan, C.C. Hegna, E.D. Held, C.C. Kim, S.E. Kruger, A.Y. Pankin, and C.R. Sovinec Phys. Plasmas **13** 058103 (2006).

[11] J. J. Ramos, Phys. Plasmas **15**, 082106 (2008)

[12] E. D. Held, J.D. Callen, C.C. Hegna, C¿R. Sovinec, T.A. Gianakon, S.E. Kruger, Phys. Plasmas **11**, 2419 (2004)

[13] T.G. Jenkins and S.E. Kruger, *submitted to Phys. Plasmas.*

[14] E.A. Belli and J.M. Candy, Plasma Phys. Cont. Fus., **51**, 5018 (2009).

[15] R.D. Hazeltine Plasma Phys. **15**, 7 (1973).

[16] B. Coppi, Phys. Fluids **7**, 1501 (1964); Biskamp, Nucl. Fusion **18**, 1059 (1978).

[17] C.R. Sovinec, J.R. King, and the NIMROD Team, J. Comp. Phys. **229**, 5803 (2010).

[18] E. Ahedo and J.J. Ramos, Nucl. Fus. **51**, 055018 (2009); V.V. Mirnov, C.C. Hegna, and S.C. Prager, Phys. Plasmas **11**, 4468 (2004).